

BESIII status and preliminary results

Xiaoyan SHEN *

Representing BESIII Collaboration

Institute of High Energy Physics, Chinese Academy of Sciences, Beijing 100049, China

E-mail: shenxy@ihep.ac.cn

The BEijing Spectrometer(BES) is a general purpose solenoidal detector located at the Beijing Electron-Positron Collider (BEPC). We report the status of BEPCII/BESIII and recent results from BESIII 100M ψ' events. These results include the measurement of h_c and χ_c , as well as the confirmation of $X(1860)$. The physics potentials of BESIII are also mentioned briefly.

XLVIII International Winter Meeting on Nuclear Physics, BORMIO2010

January 25-29, 2010

Bormio, Italy

*Speaker.

1. Introduction

The Standard Model (SM), regarded as the theory of the elementary particle physics, has been very successful in describing all the relevant physics phenomena. However, there are still many unanswered questions remained. QCD, the fundamental theory of the strong interactions, is well tested at short distances, but is not well understood at long distances because the non-perturbative effects become important. These effects are very basic to the field of particle physics and include *e.g.*, the structure of hadrons and the spectrum of hadronic states.

The Beijing Electron Positron Collider (BEPC)/Beijing Electromagnetic Spectrometer (BES) is a facility running at the energy region of 2-4.6 GeV, in which many of the charmonium states and charm mesons, as well as the τ leptons can be produced. The physics program of BES [1] covers the spectroscopy of light hadrons, charmonium physics, $D(D_s)$ physics, τ physics and precision measurement of R values. It also allows the searches for possible new physics.

Fruitful physics results have been produced with the earlier Beijing Spectrometers BES I[2] and BES II[3]. The BES I started running in 1989, and BES II is an upgraded experiment of BES I at BEPC. The precise measurement of the τ -lepton mass, performed by BES I almost twenty years ago, remains the world's best measurement of this fundamentally important quantity. The R -value measurements [4, 5, 6] from BES II have made an important improvement to the prediction of the mass of the still undiscovered Higgs boson. BES II also observed an anomalous $p\bar{p}$ threshold mass enhancement in the radiative decay $J/\psi \rightarrow \gamma p\bar{p}$ [7], an observation that has stimulated many theoretical speculations. The production of the σ and κ in J/ψ decays suggests the existence of the two controversial particles. The observation of non $D-\bar{D}$ decays of the $\psi(3770)$ by BES II also confounds theoretical expectations. At the same time, important results in this energy range have also been obtained by the CLEO-c collaboration, which include the discovery of the 1P_1 state of charmonia (the h_c) and the precise measurement of CKM matrix elements.

2. BEPCII/BESIII project

BEPCII is a major upgrade of the previous collider BEPC. In BEPC, the electrons and positrons shared the same vacuum tube in a single ring of magnets, and this arrangement limited the rate at which interesting particles are produced. The major change of BEPCII is the installation of a second ring of magnets that allows the electron and positron beams to be stored separately, and therefore leads to the designed peak luminosity of 10^{33} , an order of two improvement to that of BEPC.

The BESIII detector is designed to study the τ -charm physics and the technical requirements for a high luminosity, multi-bunch collider. Fig. 1 shows a schematic view of the BESIII detector, which is well described in ref. [8]. BESIII consists of the following components: a Helium-gas based drift chamber with a single wire resolution that is better than $120 \mu\text{m}$ and a dE/dX resolution that is better than 6%. The momentum resolution in the 1T magnetic field is better than 0.5% for charged tracks with a momentum of 1 GeV/c; a CsI(Tl) crystal calorimeter with an energy resolution that is better than 2.5% and position resolution better than 6 mm for 1 GeV electrons and gammas; a Time-of-Flight system with an intrinsic timing resolution better than 90

ps; a super-conducting solenoid magnet with a central field of 1.0 Tesla and a 9-layer RPC-based muon chamber system with a spatial resolution that is better than 2 cm.

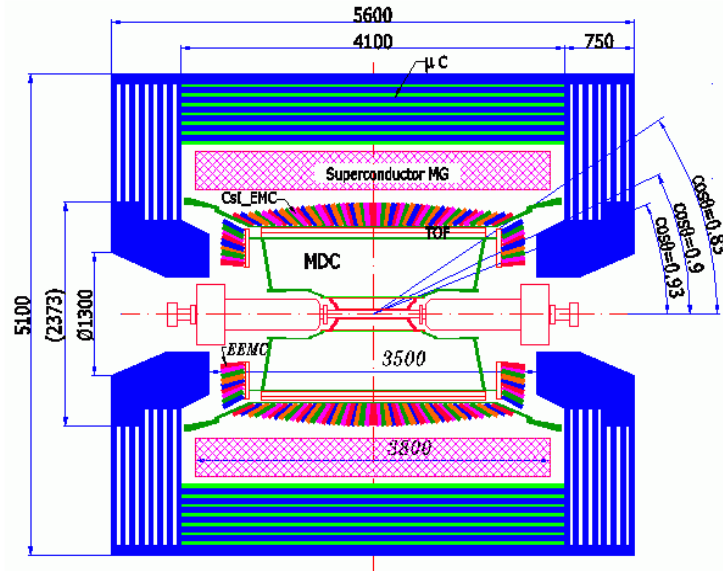


Figure 1: An Overview of the BESIII Detector.

The BESIII Offline Software System (BOSS) uses the C++ language and object-oriented techniques and runs primarily on the Scientific Linux CERN (SLC) operating system. The entire data processing and physics analysis software system consists of five functional parts: framework, simulation, reconstruction, calibration, and analysis tools.

The BOSS framework is based on the Gaudi package which provides standard interfaces and utilities for event simulation, data processing and physics analysis. The framework employs Gaudi's event data service as the data manager and the event data conversion service for conversions between persistent data and transient objects. Three types of persistent event data have been defined in the BOSS system: raw data, reconstructed data and Data-Summary-Tape (DST) data. Both reconstructed data and DST data are in ROOT format for easy management and usage. Different types of algorithms can access data from Transient Event Data Store (TEDS) via the event data service. The detector's material and geometrical information are stored in GDML files, which can be retrieved by algorithms through corresponding services.

The construction of BESIII detector started in 2003. By the end of 2007, the construction and installation of BESIII was accomplished. Cosmic ray experiments were then started and continued till March of 2008 to test each detectors, electronics, trigger, data acquisition and slow control system. In early May of 2008, BESIII was pushed into the collision point, and the precise regulation was finished at the point. The measurement showed that the location accuracy was better than the design requirements. Joint commissioning of BESIII and the accelerator began in June of 2008.

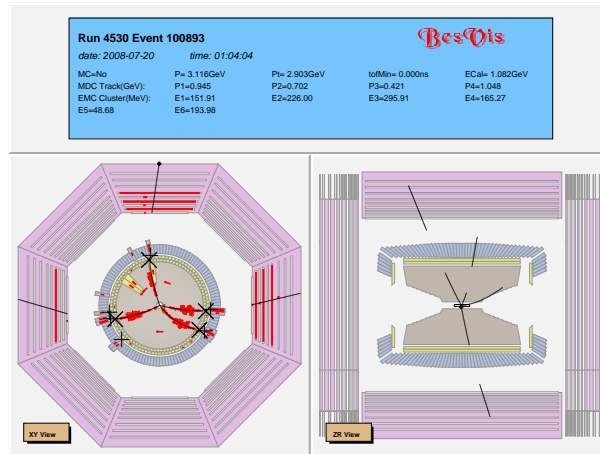


Figure 2: The first physics event recorded at BESIII.

On July 19, 2008, the first physics event produced by the electron-positron collision was observed, as shown in Fig. 2. In Nov. of 2008, about 20 pb^{-1} ψ' events were accumulated for understanding the performance of both detector and software. The detectors worked properly and stably, and the performance has reached the design requirements. The performance of the detector is shown in following table.

Detector performance

Subdetectors		design	measurement
MDC	Momentum resolution (1 GeV)	0.5-0.7%	0.58 %
	dE/dx resolution	6-8%	6.0% (hadron) 5.3% (Bhabha)
EMC	Energy resolution (1 GeV)	2.5-3%	2.5 %
	Spatial resolution	5-7 mm	6.0 mm
TOF	Time resolution	Barrel	80-90 ps 80 ps (Bhabha)
		Endcap	100-110 ps 100 ps (dimuon)
μ counter	$\delta_{R\phi}=1.4 \text{ cm} \sim 1.7 \text{ cm}$		< 1.7 cm

On March 14, 2009, BESIII finished accumulating her first large data set of over 100M ψ' events. This is the world's largest $\psi(2S)$ data set. Data taking started on March 6, 2009, after a scan of the $\psi(2S)$ peak. The J/ψ data taking started on June 12 and ended on July 28, with totally about 200M J/ψ events collected. Now, BESIII is taking data at $\psi(3770)$. Here are the recent results from BESIII 100M ψ' events.

3. Measurement of h_c in ψ' decays

Although the $c\bar{c}$ charmonium family has been studied for many years, the spin-singlet P wave charmonium state h_c was only observed in recent years by CLEOc experiment in $\psi' \rightarrow \pi^0 h_c, h_c \rightarrow \gamma \eta_c$ decays. However, the decay branching fractions of $\psi' \rightarrow \pi^0 h_c$ and $h_c \rightarrow \gamma \eta_c$, which are important in testing the theoretical models, have not been previously measured.

Using BESIII 106M ψ' events, clear h_c signals are observed for $\psi' \rightarrow \pi^0 h_c$ with and without the subsequent radiative decay $h_c \rightarrow \gamma \eta_c$ [9]. Fig. 3 shows the inclusive π^0 recoil mass spectra, where h_c signal can be clearly seen.

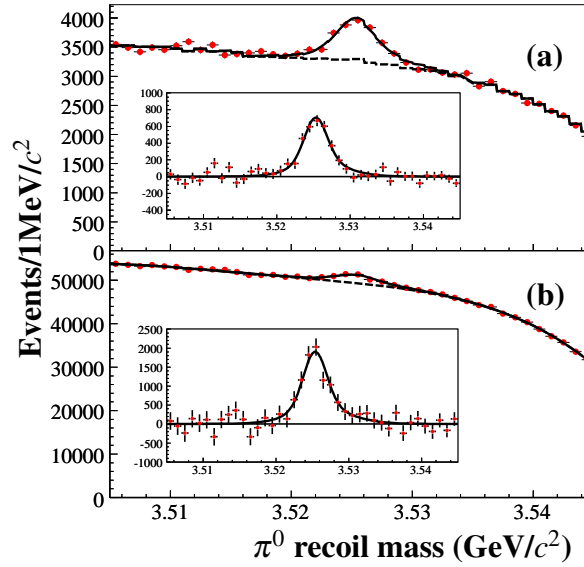


Figure 3: (a) The π^0 recoil mass spectrum and fit for the $E1$ -tagged analysis of $\psi' \rightarrow \pi^0 h_c, h_c \rightarrow \gamma \eta_c$; (b) the π^0 recoil mass spectrum and fit for the inclusive analysis of $\psi' \rightarrow \pi^0 h_c$. Fits are shown as solid lines, background as dashed lines. The insets show the background-subtracted spectra.

The π^0 recoil mass spectra (Fig. 3) are fitted by an unbinned maximum likelihood method. The results of this fit are a yield of $E1$ -tagged h_c decays of $N^{E1} = 3679 \pm 319$, where the error is statistical. The fit quality assessed with the binned distribution of Fig. 3(a) is $\chi^2/d.o.f. = 33.5/36$ (p -value 58.8%), and the statistical significance of the h_c signal is 18.6σ . The fit of the inclusive π^0 spectrum in Fig. 3 (b) is performed similarly, except that the h_c mass and width are fixed and the background is described by a 4th-order Chebychev polynomial with all parameters free. The fit result for the inclusive h_c yield is $N^{inc} = 10353 \pm 1097$, with $\chi^2/d.o.f. = 24.5/34$ (p -value 88.4%) and 9.5σ statistical significance. The insets of Fig. 3 show the π^0 recoil-mass spectra with the fitted backgrounds subtracted. The absolute branching fractions $\mathcal{B}(\psi' \rightarrow \pi^0 h_c) = (8.4 \pm 1.3 \pm 1.0) \times 10^{-4}$ and $\mathcal{B}(h_c \rightarrow \gamma \eta_c) = (54.3 \pm 6.7 \pm 5.2)\%$. A statistics-limited determination of the previously unmeasured h_c width leads to an upper limit $\Gamma(h_c) < 1.44$ MeV (90% confidence). Measurements of $M(h_c) = 3525.40 \pm 0.13 \pm 0.18$ MeV/c² and $\mathcal{B}(\psi' \rightarrow \pi^0 h_c) \times \mathcal{B}(h_c \rightarrow \gamma \eta_c) = (4.58 \pm 0.40 \pm 0.50) \times 10^{-4}$ are consistent with previous results.

4. Confirmation of $X(1860)$ at BESIII

An anomalously strong $p\bar{p}$ mass threshold enhancement, $X(1860)$, was observed by the BESII experiment in the radiative decay process $J/\psi \rightarrow \gamma p\bar{p}$ [?]. Fig. 4 is the $p\bar{p}$ invariant mass distribution, which shows a peak near $M_{p\bar{p}} = 2.98 \text{ GeV}/c^2$ that is consistent in mass, width, and yield with expectations for $J/\psi \rightarrow \gamma\eta_c$, $\eta_c \rightarrow p\bar{p}$, a broad enhancement around $M_{p\bar{p}} \sim 2.2 \text{ GeV}/c^2$, and a narrow, low-mass peak at the $p\bar{p}$ mass threshold. When an S -wave Breit-Wigner resonance function is fitted to the $p\bar{p}$ mass distribution, the peak mass is below the $p\bar{p}$ mass threshold at $M = 1859^{+3}_{-10} \text{ (stat)}^{+5}_{-25} \text{ (syst)} \text{ MeV}/c^2$ and the total width is $\Gamma < 30 \text{ MeV}/c^2$ (at the 90% C.L.). The mass and width of this resonance are not compatible with those of any known meson. The experimental observations stimulated a number of theoretical speculations, including the baryonium explanation. The confirmation of this state, the observation of more decay modes and the determination of the J^{PC} 's become crucial in clarifying the nature.

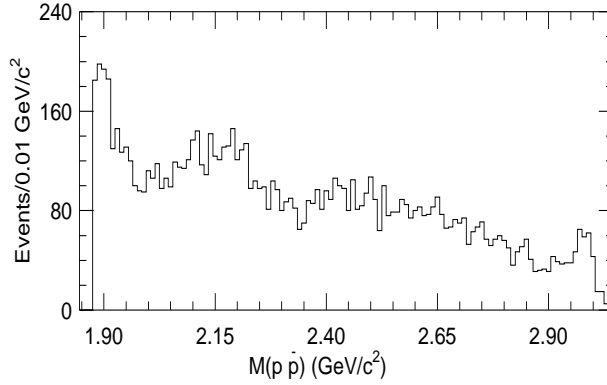


Figure 4: The $p\bar{p}$ invariant mass distribution for the $J/\psi \rightarrow \gamma p\bar{p}$ at BESII.

Using a sample of 1.06×10^8 ψ' events collected by the BESIII experiment at BEPCII, the decay channel $\psi' \rightarrow \pi^+ \pi^- J/\psi (J/\psi \rightarrow \gamma p\bar{p})$ is studied [10]. Fig. 5(a) shows the $p\bar{p}$ invariant mass distribution which has the similar features as those in Fig. 4 for BESII data, and a prominent low-mass peak at the $p\bar{p}$ mass threshold can be seen clearly. The Dalitz plot is shown in Fig. 5(b), where a band corresponding to the threshold enhancement is evident in the upper right corner. We fit it with an acceptance weighted Breit-Wigner (BW) function of the form $BW(M) \propto \frac{q^{2L+1} k^3}{(M^2 - M_0^2)^2 + M_0^2 \Gamma^2}$, where Γ is a constant (determined from fit), q is the proton momentum in the $p\bar{p}$ rest-frame, L is the $p\bar{p}$ orbital angular momentum, and k is the photon momentum, together with the function $f_{bkg}(\delta)$ with free normalization and constants a_1 and a_2 fixed at the $\pi^0 p\bar{p}$ phase-space MC values to represent the background from mis-reconstructed $\pi^0 p\bar{p}$ events and a possible non-resonant $p\bar{p}$ phase-space contribution. The BW is multiplied by the MC-determined signal acceptance that is corrected for MC and data differences of the low momentum π^+ and π^- tracking efficiencies. The tracking efficiencies determined from data are measured using samples of tagged protons and antiprotons from the process $J/\psi \rightarrow p\bar{p}\pi^+\pi^-$.

The fit yields a peak mass of $M = 1861^{+6}_{-13} \text{ (stat)}^{+7}_{-26} \text{ (syst)} \text{ MeV}/c^2$ and a narrow width that is $\Gamma < 38 \text{ MeV}/c^2$ at the 90% confidence level. These results are consistent with published BESII results.

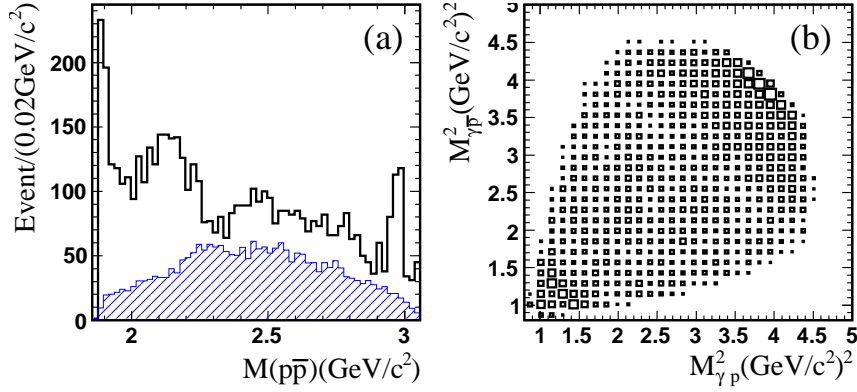


Figure 5: The $p\bar{p}$ invariant mass spectrum for the selected $\psi' \rightarrow \pi^+\pi^-J/\psi(J/\psi \rightarrow \gamma p\bar{p})$ candidate events. (a) The $p\bar{p}$ invariant mass spectrum; the open histogram is data and the hatched histogram is from a $\psi' \rightarrow \pi^+\pi^-J/\psi(J/\psi \rightarrow \gamma p\bar{p})$ phase-space MC events(with arbitrary normalization). (b) An $M^2(\gamma p)$ (horizontal) versus $M^2(\gamma\bar{p})$ (vertical) Dalitz plot for the selected events.

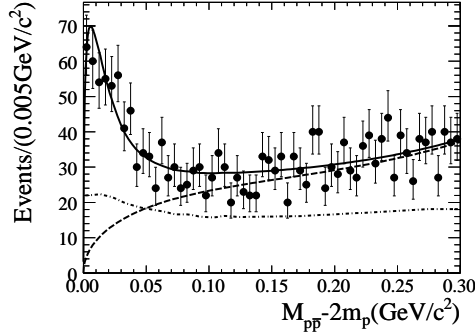


Figure 6: The $p\bar{p}$ invariant mass spectrum for the $\psi' \rightarrow \pi^+\pi^-J/\psi(J/\psi \rightarrow \gamma p\bar{p})$. The solid curve is the fit result; the dashed curve shows the fitted background function, and the dash-dotted curve indicates how the acceptance varies with $p\bar{p}$ invariant mass.

5. Measurement of χ_{cJ} decays

For χ_{cJ} states, only limited decay modes have been observed. With the large statistics of BESIII data, more χ_{cJ} decay modes can be studied and systematically measured. This is important for understanding the mechanism of charmonium decays and hadron spectroscopy. Fig.7 shows the χ_{cJ} signals in the $\omega\phi$ invariant mass spectrum in $\psi' \rightarrow \gamma\omega\phi$, and Fig. 8 shows the χ_{cJ} signals in the $\gamma\rho$, $\gamma\phi$ and $\gamma\omega$ invariant mass spectra in $\psi' \rightarrow \gamma\gamma\rho$, $\gamma\gamma\phi$ and $\gamma\gamma\omega$, respectively.

Acknowledgments

The BESIII collaboration thanks the staff of BEPCII and the computing center for their hard efforts. This work is supported in part by the Ministry of Science and Technology of China under Contract No. 2009CB825200; National Natural Science Foundation of China (NSFC) under Contracts Nos. 10625524, 10821063, 10825524, 10935007; the Chinese Academy of Sciences (CAS)

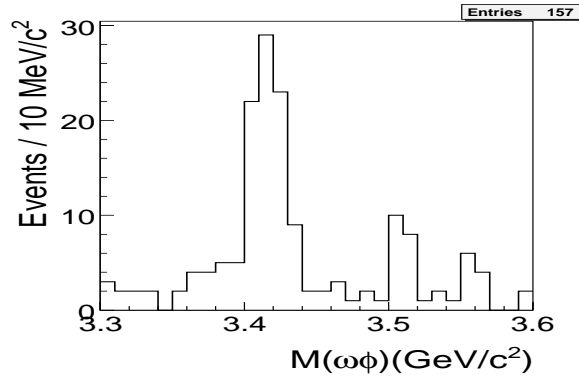


Figure 7: The $\omega\phi$ invariant mass spectrum for the $\psi' \rightarrow \gamma\omega\phi$.

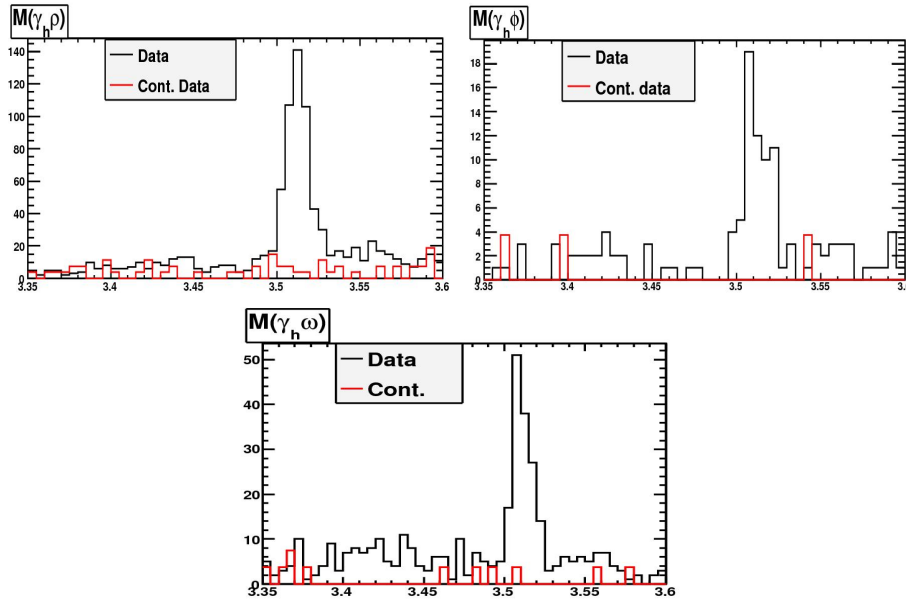


Figure 8: The γV invariant mass spectra for the $\psi' \rightarrow \gamma\gamma V$ ($V = \rho, \phi$ and ω).

Large-Scale Scientific Facility Program; CAS under Contracts Nos. KJCX2-YW-N29, KJCX2-YW-N45; 100 Talents Program of CAS.

References

- [1] D.M. Asner *et al.*, arXiv:0809.1869.
- [2] BES Collaboration (J.Z. Bai *et al.*), Nucl. Instrum. Meth. **A 344**, 319 (1994).
- [3] BES Collaboration (J.Z. Bai *et al.*), Nucl. Instrum. Meth. **A 458**, 627 (2001).
- [4] BES Collaboration (J.Z. Bai *et al.*), Phys. Rev. Lett. **84**, 594 (2000).
- [5] BES Collaboration (J.Z. Bai *et al.*), Phys. Rev. Lett. **88**, 101802 (2002).

- [6] BES Collaboration (J.Z. Bai *et al.*), Phys. Rev. Lett. **97**, 262001 (2006).
- [7] BES Collaboration (J.Z. Bai *et al.*), Phys. Rev. Lett. **91**, 022001 (2003).
- [8] BESIII Collaboration (M. Ablikim *et al.*), Nucl. Instrum. Meth. **A 614**, 345 (2010).
- [9] BESIII Collaboration (M. Ablikim *et al.*), Phys. Rev. Lett. **104**, 132002 (2010).
- [10] BESIII Collaboration (M. Ablikim *et al.*), arXiv:1001.5328, Chinese Physics **C 34(4)**, 2010.